A Calibrated Cellular Automata Model of *in vitro* Multicellular Spheroid Tumour Growth*

Monika Joanna Piotrowska[†,‡] & Simon D. Angus[§]

August 17, 2007

not for citation

Abstract

A Cellular Automata (CA) model is presented that mimics the behaviour of *in vitro* multicellular spheroid growth experiments conducted on EMT6/Ro (mammary carcinoma) cell lines as presented in [20, 22, 24]. The model represents the first stage in work that aims to compare different *in silico* modelling contexts (e.g. CAs, random diffusion, network adhesion, atomic attraction) that could be utilised to handle the specific demands of tumor cell behaviour. As opposed to several recent computational models, we explicitly couple the CA model to experimental data and show extremely good agreement across a range of outputs including bulk growth kinetics, necrotic core formation and kinetics and response to environmental glucose levels.

KEYWORDS: cellular automata; multicellular spheroid; avascular tumour; EMTG/Ro mammary carcinoma.

*This work was partially supported by the Santa Fe Institute through NSF Grant No. 0200500 entitled "A Broad Research Program in the Sciences of Complexity." This paper was prepared within the framework of the EU project "Modeling, Mathematical Methods and Computer Simulation of Tumour Growth and Therapy", MRTN - CT - 2004 - 503661.

[†]University of Witten/Herdecke, Institute of Mathematics, Stockumer Str. 10, 58448 Witten, Germany. Warsaw University.

[‡]Department of Mathematics, Informatics and Mechanics, Institute of Applied Mathematics, Banacha 2, 02 - 097 Warsaw, Poland monika@mimuw.edu.pl

[§]School of Economics, University of New South Wales, Sydney, 2052, Australia. s.angus@unsw.edu.au

1 Introduction

Medical statistics continue to reveal the fact that benign and malignant tumours are the main diseases of the XXI century and that cancer is one on the major causes of mortality the world over. For these reasons physicists, working together with scientists, have proposed an increasingly wide spectrum of mathematical models to study different kinds of malignant tumours, e.g., [1] – [3]. Of these contributions, some have focused on describing and analysing the dynamics of blood-borne tumors ([4], [5]) or soft-tissue tumors ([6] – [14]), however in both cases, the aim of mathematical models and simulations is the same – to offer a better understanding of cancer dynamics which can be used to improve therapeutic outcomes.

It is well known that the key to restoring the cancer patient to health is the early detection of neoplasmatic changes in healthy tissue. In this paper we consider this early region of of tumor growth, namely, we present a novel calibrated Cellular Automata approach to studying the growth and development of avascular, multicellular spheroids (MCS) tumours (i.e. solid symmetric tumours in the first stadium of its development).

Specifically, we propose a novel 'quasi-2D' CA model as the first stage of this work. The model is 'quasi-2D' in the sense that the tumor grows in a flat (2D) lattice of unit cells such that key calibration instruments involving concentration etc. can be meaningfully incorporated. Whilst this kind of approach has been attempted before (e.g. [15, 16]), it seems that other authors have struggled to incorporate both digital local-interactions on the lattice-site level and continuous global effects such as glucose diffusion. Moreover, although very complicated models (e.g. Zhang et al. 2007)[1] have been implemented, they have not been calibrated to experimental data, and are only now beginning this difficult process.

Furthermore, it is not clear in the literature which context is most ap-

[1] Available as a preprint online, 'Simulating Brain Tumor Heterogeneity with a Multiscale Agent-Based Model: Linking Cell Signaling, Motility Bias and Expansion Rate', accessed June 2007.

propriate for the modelling of tumor growth. The cell actions of basal metabolism, division, lysis and movement (e.g. due to soft-tissue external pressures) present unique challenges to the modeler. Specifically, the fact that existing volume (the cells) is required to produce more volume from *within* causes a considerable difficulty for CA approaches. Alternatives to this involve the computationally expensive atomic-attraction context where each cell is assumed to be globally attracted to all other cells (long-range attraction), but strongly repulsive if two cell radii over-lap (short-range repulsion). Alternatively, volume filling by random steps or utilising network spring algorithms to spread cells in a network-adhesion context are other options. Whilst we have already made considerable progress on these other contexts, we present here the initially promising results from the CA model.

In the proposed model we consider key meso-scopic and micro-scopic properties of pre-angiogenic tumour growth, namely: the diffusion of nutrients through the tissue; the consumption of nutrients by the different types of tumour cells; and the ability of the stem cell to divide in different ways (although the effects of cell heterogeneity are not reported in this paper).

We compare the result of numerical simulations with the experimental data for two-dimensional multicellular spheroids of the EMTG/Ro mouse mammary tumour line cultivated *in vitro*, which are responsible for the mammary carcinoma in breasts. The rest of the paper is organized as follows. In Section 2 we outline the description of MCS growth model. Section 3 contains the parameter estimation, numerical results and a comparison of these with reported experimental data. The current limitations and potential applications of the present model for future research can be found in Section 4.

2 Model Description

Generally, a cellular automaton is a discrete model which operates in discretized time and space. The 'world' thus being conceptualised as a grid of cells in a finite number of dimensions. Each grid-space can exist in a finite number of states and these states are updated according to a local rule, i.e.,

the state of a site in given time t depends only on the its own state in time $t-1$ and the states of its neighbours' site in time $t-1$. Normally, all sites are updated synchronously in a time step, however, in the present case, to allow for cell division and movement, subsets of sites are sometimes addressed asynchronously within an update to ensure both the legality of updates and their realism. To accurately calibrate the present 2D CA model, each lattice site does not necessarily represent a single cell (although this is possible), but instead, a filled lattice site is assumed to contain some chosen (and fixed) number of tumor cells. Although this does not allow for an arbitrary cell count (cell numbers move step-wise), it greatly enhances the range over which tumors can be modelled in this framework, and given that results below all consider a cells per site value of 200, on the scale of 1×10^5 cells, cell counts change in an approximately continuous way.

Apart from tumor cells occupying lattice sites, nutrients (in the form of glucose) can diffuse into the sites. Although glucose diffusion is a continuous processes, it can be simply discretized by applying a local updating rule as reported below.

Furthermore, since we consider a variety of effects and inputs (e.g. concentrations) in our model it does not make sense to consider the standard infinitesimally thin 2D plane. Hence, we instead consider a single sheet of 3D unit volume cells as the lattice (see Fig. 1). We refer to this methodology as a 'quasi-2D' approach.

Obviously, if the concentration of nutrients in the tissue is sufficient, the cells undertake metabolic processes to live and to proliferate. Since, the literature report that tumours can grow in an equivalently oxygen-free environment (i.e. tumours which contain cells growing under anaerobic conditions to form lactate from glucose inputs), we narrow the concept of nutrients down to glucose only. Moreover, we do not consider the metabolic waste production and its influence on cells behaviour, although this is an obvious extension as noted below.

Nutrients (glucose, at $n_e x$) are supplied to the tumor cells by an analogue

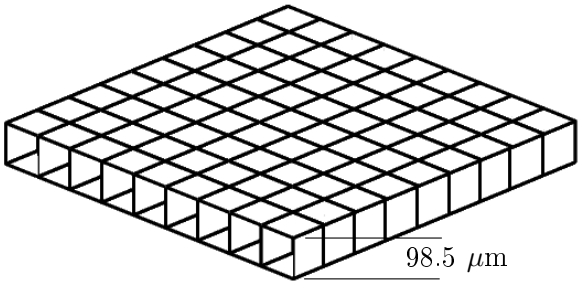

Figure 1 Example of 2-D lattice structure assumed for base context of all models. Cells inhabit positions within a unit volume site of the single layer. Lattice site side-length is calculated as described below.

of the substrate regeneration processes of *in vitro* studies. A standard 'flood' algorithm is utilised to replenish all lattice sites surrounding the tumor mass. Or in other words, we assume that sites filled with tumor cells present an impermeable layer to the substrate solution. Of course, diffusion eventually guarantees that all cells will benefit from the refreshed nutrient supply. In the present specification, nutrient replenishment occurs every time step (about every 12h).

Of course during the intensive growth tumour cells located in the centre of sphere are not sufficiently supplied by nutrients any more, and the formation of the necrotic core inside the MCS begins. Moreover, to reflect the consumption process of nutrients by cells we distinguish between the nutrient concentration in the external substrate and the glucose concentration of each cell site, see Section 3.2 for more details.

An advantage of this set-up is that although the consumption rate on a *per cell* basis is many orders of magnitude below that of the standard substrate glucose concentration (approximately 1×10^{-17} M compared with 1×10^{3} M respectively), by assuming each site contains (say) hundreds or thousands of tumor cells, various experimentally and clinically observable bulk tumor characteristics can arise in appreciable time, with a world size on the 102-10^3 scale . Indeed, if this methodology were not pursued, then the experimen-

talist would need to construct a model which contained on the order of 10^9 cells (objects) to observe phenomena of interest which, even with the fastest modern computers, is not a feasible course of action. Thus the current approach, whilst not an exact replication of the cell to cell environment allows for very facile tumor study, indeed, from mg to kg scales. Therefore, in all our models we re-scale the supply (n_{ex}) and critical (n_c) concentration as well as all diffusion (D_n) and consumption rates (C_p, C_q, C_n) of nutrients to consider a single lattice site as being occupied by some clinically relevant number of mutated cells, for detail see 3.1.

Obviously, the survival and proliferation of cells are only possible when they have a sufficient storage of nutrients or source of glucose in surrounding. Otherwise the cells will die. Therefore, in the present model we assume that each cell is able to consume slightly more (around 1%) than their basal (quiescent) consumption rate in a given time-step (assuming that this is possible given the concentration of glucose at their lattice site). Therefore, we follow each filled lattice site's nutrient level, and if this is higher than the proliferation consumption rate, then the lattice site is assumed to divide over a 12h (one step) period. As explained above, such division produces a second filled lattice site with the same number of cells inside as the parent site. Nutrients are distributed to the new lattice site cells based on a simple symmetric division of the parent sites' nutrient level post-proliferation. Of course, we do not allow cells to consume indefinitely, and set an upper limit on their cell storage of approximately 5% over their proliferation consumption rate level. Accordingly, if the cells in a filled lattice site are currently 'satisfied' (have sufficient nutrients) then the lattice site will not consume from any available glucose in that site.

To ensure the legality of the quasi-2d environment, we assume that a prospective proliferating lattice site must have an empty lattice site within its 8 near-neighbours to put the new daughter cells into. This is a more preferable approach to that of [17] – [19] who allow that the new daughter cell to be placed in the same location as the parent cell. Moreover, there

was no limitation applied as to how many daughter cells could reside in the same lattice site, which implies that it was assumed that cells could be of arbitrarily small size due to compression. Our approach is similar to that earlier proposed approaches (e.g. [15], [16]) who assume that a cell which attempts to divide would go through a search process for sufficient space for the newly generated cells beginning within nearest neighbours and expanding outwards until lattice site was found. If the search was unsuccessful within a pre-determined proliferation radius the cell would be considered non-proliferating for that time step. Although our current mechanism is more restrictive, it is the more appropriate when each lattice site contains on the order of 200 cells, since allowing a 'packet' of daughter cells of this magnitude to be transported further than near-neighbour sites does not appear appropriate.

Moreover, in our models cells can not move in an active way as was assumed in [17] – [19] where authors allowed non-proliferating cells to perform local spatial search processes within a given precision and then move there. When the mentioned precision was 100%, then tumour cells always select the best available location (based on nutrient supply) to migrate without error. The cells perform purely *random walk motion* when the precision was equal 0. Again, although this may be an experimentally observable outcome, we wish to allow any such 'movement' to arise endogenously from the model itself, rather than through an exogenously programmed regime.

We are aware that it has recently been realized that cells cultivated in the *in vivo* three-dimension (3D) like fashion behave differently from those that are kept as monolayers, see [10]. It has also been shown, that cells cultivated in 3D like conditions are rounded and show a gene expression characterisation much closer to the *in vivo* situation. Furthermore, cells need the contact with each other and have support of the extracellular matrix, which contains proteins organizing the communication between the cells as well as determining the mechanical properties of the surrounding tissue. Hence, it would seem to be natural to study and model the tissue growth in the 3D organo-

mimetic architecture. Since, the human tissue is usually organized in the three-dimensional space it is reasonable to study the 3D models rather than 2D ones. However, as with the initial *in vitro* trials which considered 2D monolayers prior to the more recent 3D analog spheroid studies, we consider the present 2D CA case, with correct calibration and reasonable assumptions to be a valuable step towards a correct 3D modelling environment, or better, as can be seen in the Results section below, to provide a very facile environment for understanding tumor growth kinetics in its own right. Furthermore, as mentioned above, the CA approach is just one of a range of approaches that could feasibly be used to model tumor growth, and it is our long-term purpose to compare each context in both 2D and 3D to aid the numerical modeling community.

3 Numerical Simulations

3.1 Model Parameters

In all presented models a 2D lattice of cells, each lattice site is assumed to be a unit-cube with side-length u and containing N cells (see Fig. 1). The value of u is calculated by taking into consideration the fact that the cell packing density (ρ) through the growth period is estimated to be equal $3 - 5 \times 10^8$ cell per cm^3, [20]. Based on this result and taking $\rho = 4 \times 10^8$ c.cm^{-3} first we calculate the volume (V_{cells}) occupied by N cells $V_{cells} = \frac{N}{\rho} \times 10^{12}$ μm^3 and then assuming that the lattice site length is equal to the diameter of a sphere with volume V_{cells} we obtain following formula

$$u = 2\left(\frac{3}{4\pi}V_{cells}\right)^{\frac{1}{3}} \quad (1)$$

$$= 2\left(\frac{3N}{4\pi\rho}\right)^{\frac{1}{3}} \times 10^4 \ \mu\text{m}. \quad (2)$$

Secondly, the time step, Δt, for all simulations is chosen to be equal to the whole cell cycle duration, which in an exponentially growing monolayers cell culture takes around 12 h, see [21] or [22]. Thus, by taking the time-step to

be 12 h, the single parameter of control for all subsequent rescaling is the number of cells per lattice site, n. This choice, along with the time-step Δt then allows a full re-scaling of volumetric and time-dependent (e.g. rate) calculations.

Recent research has found that glucose concentrations below 2.5 mM provide extremely difficult conditions for many cancer cell lines, we have assumed for all presented models that $n_c = 2.5$ mM is the critical concentration of nutrients. If the concentration of nutrients is higher or lower than n_c, then cells are able to remain in a quiescent (or proliferating) state or undergo apoptosis/necrosis, respectively. Taking into account data given in [20], we have assumed that the concentration of glucose in the medium (n_{ex}) is in a range from 0.4 to 16.5 mM for data reported in the last study below, but for all other studies, is assumed to be 5.5 mM.

Again in [20] the glucose and oxygen uptake for multicellular spheroids of the EMTG/Ro tumour line were measured. The experimental data presented in [20], Table 2 shows that reducing the glucose concentration rate from normal to near zero, while maintaining the oxygen concentration constant at 0.28 mM. These data indicate that non-cycling (plateau-phase) EMTG/Ro cells have reduced metabolic rates of oxygen and glucose consumption compared with exponentially-growing cells, for details see Table 5 in [20]. Hence, assuming that necrotic cells do not consume (in fact, we assume necrotic lattice sites disappear without waste) and taking into account the consumption rates $C_p = 18 \times 10^{-17}$, $C_q = 15 \times 10^{-17}$, $C_n = 0$ Mc^{-1}s^{-1} for proliferating, quiescent and necrotic cells, respectively, we can calculate the consumption rates per lattice site per time step (12 h) as follows,

$$\begin{aligned} C_p^{site} &= 1.24 \times 10^{-18} \text{ mol.u}^{-3}.(\text{site}.\Delta\text{t})^{-1} \quad , \\ C_q^{site} &= 1.49 \times 10^{-18} \text{ mol.u}^{-3}.(\text{site}.\Delta\text{t})^{-1} \quad , \\ C_n^{site} &= 0 \text{ mol.u}^{-3}.(\text{site}.\Delta\text{t})^{-1} \quad . \end{aligned}$$

Casciari, at al., [23], have experimentally estimated effective diffusivity of glucose of mouse (EMT6/Ro) and human tumour (colon and squamous

carcinoma) cell lines, by the efflux of tritium labelled L-glucose from 2D cultivated spheroids with time. The effective diffusion coefficient for EMT6/Ro MSCs were estimated to be equal to $10.5 \pm 2.3 \times 10^{-7}$ $\mathrm{cm}^2.\mathrm{s}^{-1}$and it was highest among all investigated cell lines. Thus, according to the assumed diffusion constant $D_n = 10.5 \times 10^{-7}$ $\mathrm{cm}^2.\mathrm{s}^{-1}$, the packing-density $\rho = 4 \times 10^8$ $\mathrm{c.cm}^{-3}$ (estimated in [20]) and choice of $N = 200$ cells per lattice site, one obtains: $D_n = 1.08 \times 10^{-2}$ $\mathrm{u}^2.\mathrm{s}^{-1}$.

However, since each model time-step is set to $\Delta \mathrm{t} = 12$ h, it remains to convert this diffusion coefficient into a meaningful estimate of diffusion across a 12 h (rather than 1 s) period. To begin, in the model, diffusion is modelled numerically by the standard discretized diffusion equation,

$$n_0^{t+1} = n_0^t(1-p) + \sum_{j \in \mathcal{N}^0} p\frac{n_j^t}{8}, \tag{3}$$

where p is the fraction of a site's nutrients to share with surrounding sites, and $\mathcal{N}^0$ is the set of sites in site 0's Moore neighbourhood. That is, a component of the nutrients at n_0^t remain after distribution to surrounding cells, plus nutrients are gained from a similar process due to site 0's neighbours. The factor 8 is used to distribute this amount evenly amongst the neighbours of site 0. This process can be shown to be analogous to Fick's 1st Law of Flux. Define by $\langle n_1^t \rangle$ the average nutrient level of sites surrounding site 0, and we obtain,

$$n_0^{t+1} = n_0^t(1-p) + p\langle n_1^t \rangle \quad , \tag{4}$$

which can be re-written,

$$n_0^{t+1} = n_0^t + p(\langle n_1^t \rangle - n_0^t) \quad , \tag{5}$$

Rearranging to find the first difference,

$$(n_0^{t+1} - n_0^t) = p(\langle n_1^t \rangle - n_0^t) \quad . \tag{6}$$

One finds that the flux in nutrients across the adjoining lattice walls is proportional to the difference in concentration between the lattice site and its

neighbours. Indeed, the fraction p is analogous to the diffusion coefficient defined above.

To sum up this section, the parameters used in the model are collected in Table 1. As noted above, with the quasi-2D lattice-approach to the CA modelling context, one can directly correlate experimental quantities with the numerical computation environment. Indeed, the modeller need only choose the number of cells per lattice site (N) and a re-scaling procedure will generate all model parameters in lattice and time-step model units. Furthermore, as mentioned above, although the present model is aligned to the EMT6/Ro cell line for verification purposes, a broad range of tumor and substrate contexts can be reproduced within the modelling set-up by changing the input parameters.

Table 1 Summary of Control Parameters (with references) and Calculated Parameters used in the simulations.

Description	**Symbol**	**Value**	**Units**
Control Parameters			
Cell packing density [20]	ρ	4×10^8	$\mathrm{c.cm^{-3}}$
Tissue glucose conc. [20]	n_{ex}	5.5	mM
Quiescent consumption rate per site [20]	C_q	15×10^{-17}	$\mathrm{M.(c.s)^{-1}}$
Proliferating consumption rate per site [20]	C_q	18×10^{-17}	$\mathrm{M.(c.s)^{-1}}$
Glucose diffusion coef. [23]	D_n	10.5×10^{-7}	$\mathrm{cm^2.s^{-1}}$
Time step [21, 22]	Δt	12	h
Cells per site (set)	N	200	$\mathrm{c.site^{-1}}$
Calculated Parameters			
Unit side-length	u	98.5	μm
Tissue glucose conc.	n_{ex}	5.25×10^{-9}	$\mathrm{mol.u^{-3}}$
Quiescent consumption rate (per site)	C_q	1.24×10^{-18}	$\mathrm{mol.u^{-3}.(site.\Delta t)^{-1}}$

(table continued on next page ...)

Table 1 Parameters (continued from previous page)

Description	Symbol	Value	Units
Proliferating consumpiton rate (per site)	C_p	1.49×10^{-18}	$\mathrm{mol.u^{-3}.(site.\Delta t)^{-1}}$
Glucose diffusion coef.	D_n	0.0108	$\mathrm{u^2.s^{-1}}$

3.2 Results

To investigate the model, results are presented for conditions as close to that of the study of EMT6/Ro cells reported in [20] as possible. This study (and others by the same group) was chosen for comparison since although the data reported are largely for spheroids as opposed to monolayers, many of the salient features of the growth kinetics are comparable across the different geometries. A 'substrate' glucose concentration of 5.5mM was chosen for initial trials as reported below with a constant oxygen concentration of 0.28 mM in mind (although we do not explicitly model oxygen diffusion).

An example model visualisation is given in Fig. 2 which shows the initial 'substrate' lattices sites set to n_{ex} and the seed lattice positions filled with growing tumour cells. In this case (as below) each lattice site (black pixel) contains 200 cells. The cells spread outward in the lattice arrangement as they divide. In the third row, the beginning of a visible necrotic core can be seen, which spreads to a significant portion of the growing tumour sheet after 12 days (bottom).

To obtain quantitative results, the model was run for 30 time-steps, or the equivalent of 15 days, each run taking less than 1min of CPU time to complete. The diameter and cell count of the spreading tumor mass was calculated, and after scaling conversion, gave rise to the plots in Fig. 3. As can be seen, the Model reproduces common, and well-documented features of tumour growth. Namely, the linear diameter growth relationship, as shown in [20] and the Gompertzian cell count (or cell volume) curve. The non-linear fit to the data was performed by the standard MATLAB `fminsearch`

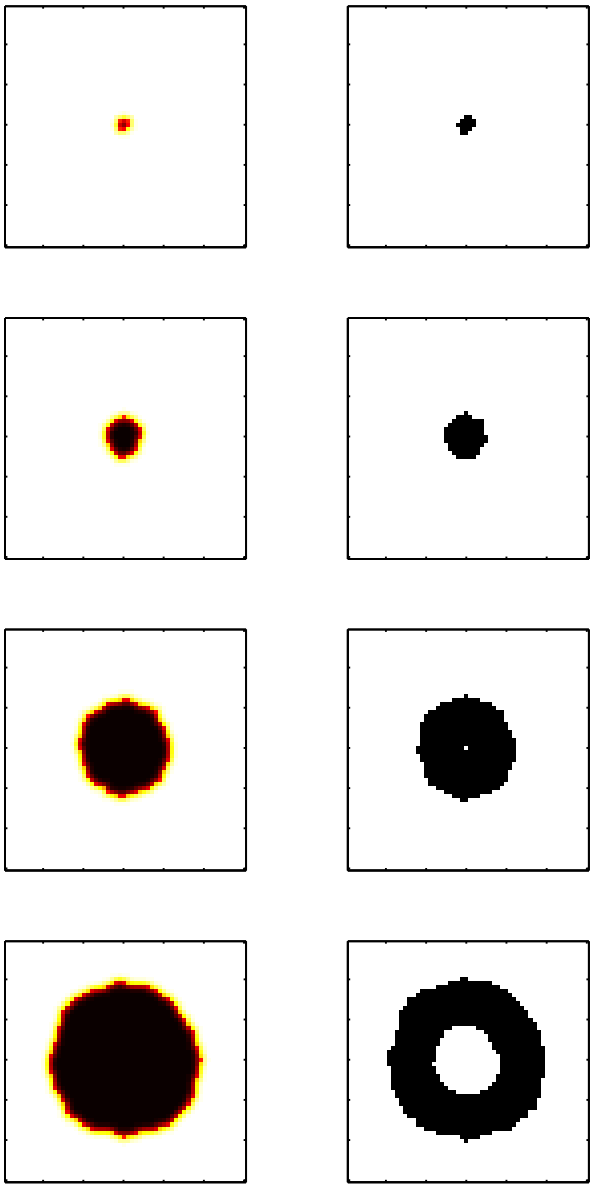

Figure 2 Example images from a Model run under typical conditions. (left) Nutrients color-coded such that white equates with n_{ex}; and (right) Filled lattice sites (black). Images taken at the equivalent of 2, 4, 8, and 12 days respectively (top to bottom). The box side-length is approximately 591μm.

procedure with a squared log-residual error function. Parameters for this fit are given in the caption, and indicate an initial cell population of 182, which is very close to the actual seed of 200 cells in the first lattice site, and an initial doubling time of 9.51 h, which happens to be almost exactly the same as the 9.5 h reported in [24, p.2434] for EMT6/Ro monolayer growth.

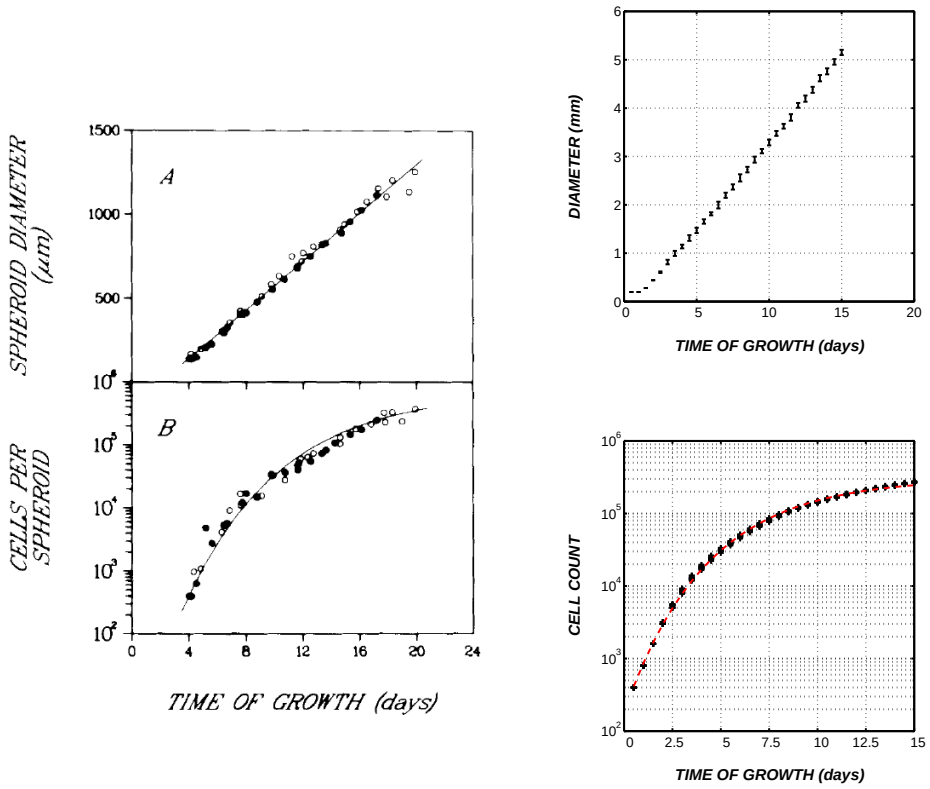

Figure 3 Experiment (left, reproduced from Fig. 1, [20]) and model output (right) for growth diameter and total (live) cells. Points represent mean of 10 trials at $n_{ex} = 5.5$mM, error bars show standard deviations. The dashed line for model cell-count is a nonlinear least squares best fit of all points to the Gompertz growth model ($N_0 = 182, A = 0.874, B = 0.118$).

Moving to the development of the necrotic core, data presented in [20] indicates in increase necrotic core volume as a fraction of total spheroid

volume. Once a necrotic core had developed in the model tumours, data were gathered in a similar way. Fig 4 shows an apparently linear relationship between necrotic volume fraction and tumour diameter in accordance with the experimental data. Indeed, for a 1.6 fold increase in spheroid diameter, the experimental study indicated that necrotic volume fraction increased from 12 to 38 percent. In the case of the model, and equivalent increase in diameter (approx. 3mm to 5mm) gave rise to an approximate change in necrotic volume fraction from 2 to 25 percent.

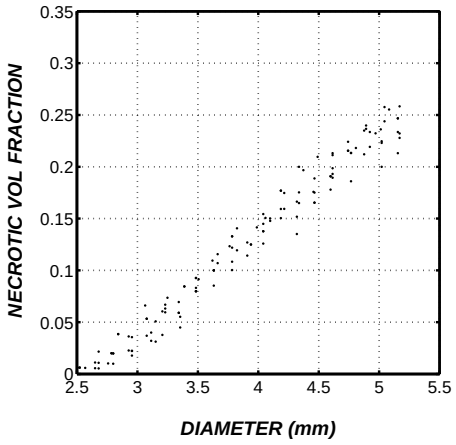

Figure 4 Necrotic core 'volume' fraction as a function of growth diameter. All points where the fraction was greater than zero from 10 trials are given. Compare Table 3 in [20].

Finally, pushing the model further, a study of several glucose concentrations for the substrate layer was conducted along the lines of that reported in [25]. Glucose concentrations ranging from 0.4mM to 16.5mM were studied over 10 simulations with other parameters as above. Fig 5 shows the results of this trial compared to the experimental findings for comparison. Again, although the experimental work was conducted on tumour spheroids, the positive relationship was recovered in the model over a significant range of viable cell rim thicknesses.

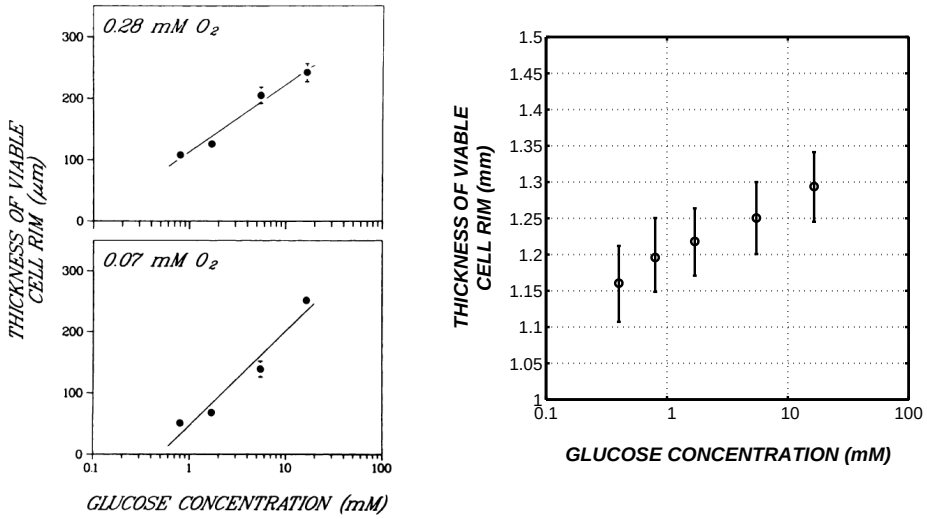

Figure 5 Experiment (left, reproduced from Fig. 4, [25]) and Model output (right) for thickness of the viable rim as a function of glucose concentration as used in the reference (16.5 mM, 5.5 mM, 1.7 mM, 0.8 mM, 0.4 mM).

4 Discussion

This paper has presented a fully calibrated quasi-2D model of avascular tumor growth, focusing, for the purpose of example, on the EMTG/Ro mammary carcinoma cell line. The model effectively takes into consideration the state of each cell depending not only on local rules due to the lattice site micro-environment but also on the concentration of nutrients which diffuse from the substrate region. As the results in Fig 2 to 4 attest, the present model faithfully reproduces key bulk features of tumor development, including Gompertzian growth kinetics and necrotic core development whilst also providing calibrated, and in some cases very accurate estimates of experimental data. Furthermore, although only one trial is reported in this paper, the substrate glucose variation trial reported in Fig. 5 provides very encouraging analogs with that of the experimental data reported in [25].

Whilst these present results are very encouraging and stand apart from other computational models in the literature which do not so faithful report

calibrated behaviour and measures, the model is still in its infancy. There is much for future work to handle. For instance, without additional terms describing the cell cycle, the present model is not able to reflect the influence of sub-cellular levels of tumour development. Some progress on this front has already been attempted however, with cell heterogeneity via symmetric (stem) or asymmetric (stem, and differentiated) cell division already explicitly modelled (though not quantitatively reported here). Fig 6 shows an image taken from this kind of set-up and thus with further analysis will be able to shed interesting light on cell-type questions and locations that are difficult to experimentally answer at present.

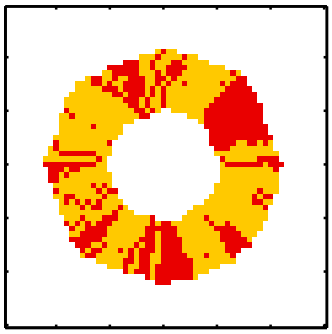

Figure 6 Example model run under heterogeneous division. Probability of asymmetric division 0.95. Colours indicate stem (yellow) and differentiated (red) cell.

In future we would like to include the production of growth (e.g., transforming growth factor) and inhibitory factors, produced by cells, as well as waste metabolic products (e.g., lactate) or oxygen tension. The model in the present version does not take account that non-cycling cells have a smaller cell volume ($2.2 \pm 0.29 \times 10^9$ cm^3) than the proliferating ones ($3.0 \pm 0.17 \times 10^9$ cm^3). However, this will be updated in the future.

Furthermore, work has already begun on updating the present model which is based on the *in vitro* context, to that of the *in vivo* context, some-

thing that is not currently reported in the literature. To this end, instead of the substrate 'flood' technique, capillary end-points are incorporated into the lattice world, and allowed to expand around the growing tumor. And finally, given the standardized set-up of the quasi-2D case, the CA model here presented is to be extended into a true 3D model, but retaining the unit-volume lattice approach.

Finally, as was noted in the introduction, this model completes the first stage of a comparative study of different numerical simulation contexts. It is hoped that such detailed calibration to experimental findings will greatly improve our understanding of the *in silico* approach such that findings and predictions from these models will be of most help to experimentalists and clinicians in tackling this most devastating of diseases.

References

[1] Cancer modeling and simulation, (Edited by L. Preziosi), Chapman & Hall/CRC, (2003).

[2] N. Bellomo, G. Forni: Dynamics of tumour interaction with the host immune system. *Math. Comp. Model.* **20** (1994) 107-122.

[3] R.A. Gatenby, T.L. Vincent and R.J. Gillies, Evolutionary dynamics in carcinogenesis. *Math. Mod. Meth. Appl. Sci.* **15** (2005) 1619-1638.

[4] L.K. Andersen, M.C. Mackey: Resonance in periodic chemotherapy: A case study of acute myelogenous leukemia. *J. Theor. Biol.* **209** (2001) 113-130.

[5] H. Moore, N. K. Lib: A mathematical model for chronic myelogenous leukemia (cml) and t cell interaction. *J. Theoret. Biol.* **227** (2004) 513-523.

[6] H. Hatzikirou, A. Deutsch, C. Schaller, M. Simon: Mathematical modelling of glioblastoma tumour development: A review. *Math. Mod. Meth. Appl. Sci.* **15** (2005) 1779-1794.

[7] M. Bodnar, U. Foryś: Time delays in regulatory apoptosis for solid avascular tumour. *Math. Comp. Model.* **37** (2003) 1211-1220.

[8] H. M. Byrne, M. A. J. Chaplain: Growth of non-nerotic tumours in the presence and absence of inhibitors. *Math. Biosci.* **130** (1995) 151-181.

[9] M.J. Piotrowska, U. Foryś: Time Delays in Avascular Tumour Growth. *Proceedings of the Tenth National Conference on Application of Mathematics in Biology and Medicine*, Święty Krzyż, 22-25 September 2004.

[10] M.J. Piotrowska: Hopf bifurcation in a solid avascular tumour growth model with two discrete delays. *Math. Comp. Model.* (article in press)

[11] M.A.J. Chaplain, M. Ganesh, I.G. Graham: Spatio-temporal pattern formation on spherical surfaces: Numerical simulation and application to solid tumour growth, *J. Math. Biol.* **42** (2001) 387-423.

[12] M.A.J. Chaplain: Avascular growth, angiogenesis and vascular growth in solid tumours: The mathematical modelling of the stages of tumour development, *Math. Comp. Model.* **23** (1996) 47-87.

[13] H.M. Byrne, M.A.J. Chaplain: On the role of cell-cell adhesion in models for solid tumour growth, *Math. Comp. Model.* **24** (1996) 1-17.

[14] M. Bodnar, U. Forys: Time delay in necrotic core formation, *Math. Biosci. & Eng.* **2** (2005) 461-472.

[15] A.R. Kansal, S. Torquato, G.R. Harsh Iva, E.A. Chioccaeb, T.S. Deisboeck: Simulated Brain Tumor Growth Dynamics Using a Three-Dimensional Cellular Automaton. *J. theor. Biol.* **203** (2000) 367-382.

[16] A. R. Kansal, S. Torquato, E.A. Chioccaeb, T.S. Deisboeck: Emergence of a Subpopulation in a Computational Model of Tumor Growth. *J. theor. Biol.* **207** (2000) 431-441.

[17] Y. Mansury, M. Kimura, J. Loboz, T.S. Deisboeck: Emerging Patterns in Tumor Systems: Simulating the Dynamics of Multicellular Clusters with an Agent-based Spatial Agglomeration Model. *J. theor. Biol.* **219** (2002) 343Ű370.

[18] Y. Mansury, T.S. Deisboeck: Simulating 'structureŰfunction' patterns of malignant brain tumors. *Physica A* **331** (2004) 219 Ű 232.

[19] Y. Mansury, T. S. Deisboeck: The impact of 'search precision' in an agent-based tumor model. *J. theor. Biol.* **224** (2003) 325Ű337.

[20] J.P. Freyer, R.M. Sutherland: A Reduction in the In Situ Rates of Oxygen and Glucose Consumption of Cells in EMT6/Ro Spheroids During Growth. *JOURNAL OF CELLULAR PHYSIOLOGY* **124** (1985) 516-524.

[21] Y. Jiang, Jelena Pjesivac-Grbovic, Charles Cantrell, and James P. Freyer: A Multiscale Model for Avascular Tumor Growth. *Biophysical Journal* **89** (2005) 3884-3894.

[22] J.P. Freyer, R.M. Sutherland: Selective dissociation and characterization of cells from different regions of multicell tumor spheroids. *Cancer Res.* **40** (1980) 3956-3965.

[23] Joseph J. Casciari, Stratis V. Sotirchos, and Robert M. Sutherland: Glucose Diffusivity in Multicellular Tumor Spheroids. *Cancer Res.* **48** (1988) 3905-3909.

[24] J.P. Freyer: Role of Necrosis in Regulating the Growth Saturation of Multicellular Spheroids, *Cancer Res.* **48** (1988) 2432-2439.

[25] J.P. Freyer, R.M. Sutherland: Regulation of Growth Saturation and Development of Necrosis in EMT6/Ro Multicellular Spheroids by the Glucose and Oxygen Supply, *Cancer Res.* **46** (1986) 3504-3512.